

The radio core and jet in the broad absorption line quasar PG 1700+518

J. Yang^{1*}, F. Wu^{2,3}, Z. Paragi^{1,4} and T. An^{2,5,6}

¹*Joint Institute for VLBI in Europe, Postbus 2, 7990 AA Dwingeloo, The Netherlands*

²*Shanghai Astronomical Observatory, CAS, 200030 Shanghai, P.R. China*

³*Graduate University of the Chinese Academy of Sciences, 100049 Beijing, P.R. China*

⁴*MTA Research Group for Physical Geodesy and Geodynamics, POB 91, H-1521 Budapest, Hungary*

⁵*Key Laboratory of Radio Astronomy, Chinese Academy of Sciences, P.R. China*

⁶*Netherlands Institute for Radio Astronomy (ASTRON), Postbus 2, 7990 AA Dwingeloo, The Netherlands*

Accepted 2011 Oct. Received 2011 Oct. ; in original form 2011 Oct. xx

ABSTRACT

The blue-shifted broad absorption lines (BAL) or troughs are observed in Active Galactic Nuclei (AGNs) when our line of sight is intercepted by a high speed outflow (wind), likely originating in the accretion disc. The outflow or wind can shed light on the internal structure obscured by the AGN torus. Recently, it has been shown that this outflow is rotating in the BAL quasar PG 1700+518, further supporting the accretion disc origin of the wind. With the purpose of giving independent constraints on the wind geometry, we performed high-resolution European VLBI Network (EVN) observations at 1.6 GHz in 2010. Combining the VLBI (Very Long Baseline Interferometry) results with the Very Large Array (VLA) archival data at 8.4 GHz, we present its jet structure on scales of parsec (pc) to kiloparsec (kpc) for the first time. The source shows two distinct jet features in East-West direction with a separation of around 4 kpc. The Eastern feature, which has so far been assumed to hide the core, is a kpc-scale hot spot, which is completely resolved out in the EVN image. In the western jet feature, we find a compact jet component, which pinpoints the position of the central black hole in the galaxy. Jet components on both sides of the core are additionally detected in the Northwest-Southeast direction, and they show a symmetric morphology on scale of <1 kpc. This two-sided jet feature is not common in the known BAL quasars and indicates that the jet axis is far away from the line of sight. Furthermore, it is nearly parallel to the scattering plane revealed earlier by optical polarimetry. By analogy to polar-scattered Seyfert 1 galaxies, we conclude that the jet likely has a viewing angle around 45°. The analogy is further supported by the recent report of significant cold absorption in the soft X-rays, a nearly unique feature to polar-scattered Seyfert galaxies. Finally, our observations have confirmed the earlier finding that the majority of radio emission in this galaxy arises from AGN activity rather than star-formation.

Key words: galaxies: active – galaxies: jets – galaxies: individual: PG 1700+518 – radio continuum: galaxies.

1 INTRODUCTION

Broad absorption line (BAL) quasars constitute a significant fraction, ~ 15 percent, in the entire quasar population (e.g. Trump et al. 2006). It is generally believed that their broad absorption lines are an indication of a high-velocity outflow or wind (e.g. Axon et al. 2008). In the BAL quasar PG 1700+518 (J1701+5149) it was found by Young et al.

(2007) that the broad Balmer lines show not only radial motion but also significant rotation ($\sim 4000 \text{ km s}^{-1}$), indicating that the outflow is related to a rotating accretion disc wind. The geometry of this outflow thus is of high interest because it may shed light on the innermost structure of active galactic nucleus (AGN) itself in this system.

Assuming that both the accretion disc and the torus have the same axis as the jet in PG 1700+518, high resolution radio observations of the jet can provide constraints on the wind geometry. The jet axis is perpendicular to the

* E-mail: yang@jive.nl

polarisation position angle of optical continuum emission in most Seyfert 2 galaxies and parallel in around three quarter of Seyfert 1 galaxies (e.g. Antonucci 1983; Smith et al. 2004). These polarisation properties can be well explained within the model of two scattering regions (Smith et al. 2004; Axon et al. 2008). The scattered emission is dominated by polar scattering in Seyfert 2 galaxies, and by equatorial scattering in Seyfert 1 galaxies. The transition between Type 1 and 2 Seyfert galaxies is polar-scattered Seyfert 1 galaxies. In this case our line of sight is right along the edge of the torus, thus the polarized light from the equatorial scattering region is sufficiently suppressed, while the broad wings of the Balmer lines are not affected.

The quasar PG 1700+518 was first discovered by Schmidt & Green (1983) in an optical survey and later identified by Wampler (1985) as a rare, nearby BAL quasar. It is an ultra-bright ($m_R \sim 15.5$) infrared source, while its host galaxy is one of the most molecular gas-rich Palomar-Green QSO hosts. The star-forming molecular gas mass was estimated to be $\sim 6 \times 10^{10} M_\odot$ from CO(1 \rightarrow 0) emission observations (Evans et al. 2009). A ring-shaped companion galaxy was found in deep infrared observations (Stockton et al. 1998) at 1.6 arcsec North of the quasar with a similar redshift ($z \sim 0.29$), indicating a merging process between the two galaxies.

The radio counterpart of PG 1700+518 is weak. It has a total flux density of 20 ± 1 mJy at 1.4 GHz (e.g. Barvainis & Lonsdale 1996). The source is not clearly resolved with the Very Large Array (VLA) below ~ 5 GHz. At higher frequencies the source shows two extended emission regions, separated by ~ 1 arcsec (4 kpc) in the East-West direction (Hutchings et al. 1992; Kukula et al. 1998; Kellermann et al. 1994). VLA images at 8.4 GHz (Kukula et al. 1998) reveal that the western emission region extends towards North-West. Blundell & Beasley (1998) reported a possible detection in the western emission region with the Very Long Baseline Array (VLBA) at 8.4 GHz, but only at the 3σ level and with no information on the jet axis.

The letter is organised in the following sequence. We introduce our observations and data reduction in Section 2 and then present the imaging results in Section 3. Based on these high-quality images, we identify the radio core, present the case that the quasar is a polar-scattered Seyfert 1-like object, and discuss the discrepancy between the radio and infrared-derived star-formation rates in Section 4. Finally, we summarise our results in Section 5. Throughout this paper, we used the cosmology corrected scale: 4.2 pc mas^{-1} at $z = 0.29$, derived from the following cosmology: $H_0 = 73 \text{ km s}^{-1} \text{ Mpc}^{-1}$, $\Omega_M = 0.27$ and $\Omega_\Lambda = 0.73$.

2 OBSERVATIONS AND DATA REDUCTION

2.1 The 1.6 GHz EVN observations

The Very Long Baseline Interferometry (VLBI) observations of PG 1700+518 were performed at 1.6 GHz with the European VLBI Network (EVN) on 2010 November 5 (project code: EY012). There were nine stations (Effelsberg, Westerbork in the phase-array mode, Jodrell Bank (MkII), Onsala, Medicina, Torun, Svetloe, Zelenchukskaya, Badary) participating in the experiment. Since PG 1700+518 is not a bright

radio source, we adopted the phase-referencing technique with a cycle time of 6 minutes: 2 minutes on the calibrator and 4 minutes on the target. The reference calibrator J1701+5133 is quite close (15 arcmin) to our target and has a compact and bright core in the VLBA Imaging and Polarisation Survey (VIPS, Helmboldt et al. 2007). The adopted J2000 coordinate (Petrov & Taylor 2011) of the reference source is RA = $17^{\text{h}}01^{\text{m}}22^{\text{s}}.34991$, Dec. = $+51^{\circ}33'49''.6890$. The EVN observations lasted for 6 hours totally, and used a recording rate of 512 Mbps (dual polarisation, 16 channels, 8 MHz per channel, 2-bit sampling). Correlation was done with the EVN MkIV Data Processor at JIVE (Joint Institute for VLBI in Europe) with an integration time of 2 seconds and 16 frequency points per channel.

Following the online EVN data reduction guide, the *a-priori* calibration was done in AIPS (Astronomical Image Processing System; Greisen 2003). The correlation amplitudes were calibrated using the measured gain curves and system temperatures for most of the telescopes; we used nominal SEFDs (System Equivalent Flux Density) for Badary, Jodrell Bank, Svetlo and Zelenchukskaya. Fringe-fitting was done in two steps: first we removed the instrumental inter-channel delay using a two-minute scan of the bright calibrator J1638+5720 (“manual phasecal”), and then we solved for all the delay, delay-rate and phase solutions of calibrators via global fringe-fitting of the whole experiment. The phase solutions of PG 1700+518 came from linear interpolation of calibrator solutions. Bandpass calibration was done using J1638+5720. Finally, the data were averaged in each subband and split into single-source files.

Self-calibration and imaging were done in the Caltech software package Difmap (Shepherd et al. 1994). The phase-reference source J1701+5133 was imaged first. It has a total flux density of 55 mJy, dominated by a compact core (92% of the total flux density). The final amplitude and phase self-calibration was done in AIPS using the calibrator image obtained in Difmap. Both the amplitude and the phase solutions were applied to the target source. There was no self-calibration applied during the imaging of PG 1700+518. Furthermore, we did circular Gaussian model fitting in Difmap (Shepherd et al. 1994) to determine the characteristic parameters of each discrete emission region. The model-fitting results are summarised in Table 1.

2.2 The 8.4 GHz VLA archive data

We analysed a VLA data set (project code: AB0512), which was available in the NRAO Data Archive. The source PG 1700+518 was observed with the VLA in configuration A at 8.4 GHz for ~ 2.3 hours on 1988 December 15. The absolute flux density was calibrated with 3C 286. The nearby point source 1739+522 was used to further calibrate the amplitude and phase. The final imaging was done without any self-calibration in Difmap (Shepherd et al. 1994).

3 EVN AND VLA IMAGING RESULTS

The final EVN and VLA imaging results are collected in Fig. 1. The left VLA image shows that PG 1700+518 has two jet features, marked as E and W and separated by 912 ± 3 mas, in agreement with the earlier imag-

Table 1. The results of the circular Gaussian model fitting for the jet features in PG 1700+518. Note that component C (core) is the reference origin and the last column is total flux density.

Array	Freq. (GHz)	Comp.	Radius (mas)	P.A. ($^{\circ}$)	Size (mas)	Flux (mJy)
VLA	8.4	C	0 ± 0		<30	0.87 ± 0.09
VLA	8.4	NW	215 ± 3	-32.2 ± 0.8	134 ± 3	0.44 ± 0.05
VLA	8.4	SE	228 ± 4	141.1 ± 1.0	139 ± 4	0.35 ± 0.04
VLA	8.4	E	912 ± 3	93.6 ± 0.2	203 ± 3	1.69 ± 0.17
EVN	1.6	C	0 ± 0		3 ± 1	1.9 ± 0.2
EVN	1.6	NW	231 ± 2	-39.0 ± 0.6	>40	>1.6
EVN	1.6	SE	270 ± 2	133.3 ± 0.6	>40	>1.5

ing results (Hutchings et al. 1992; Kellermann et al. 1994; Kukula et al. 1998). Compared with their images, our image has the better resolution: a nearly circular beam with a size of 0.25 arcsec. The eastern feature has a peak brightness of $0.99 \text{ mJy beam}^{-1}$, slightly higher than the western one. In addition, there is a hint of surrounding diffuse emission (cf. Hutchings et al. 1992) at the 4σ level ($1\sigma=0.012 \text{ mJy beam}^{-1}$). The western jet feature is elongated along the SE-NW direction (cf. Kukula et al. 1998). With three circular Gaussian components (SE, C and NW), the elongated structure can be well fitted.

The right panel in Fig. 1 is the EVN image which was restored with a 30 mas circular Gaussian, to present the faint, resolved components better (indicated by SE, C, and NW). The inset shows the full resolution map of the brightest feature. Note that the components SE and NW are too extended to be seen with a beam of <10 mas, and their total flux density and size in Table 1 are underestimated due to the absence of short baselines (<200 km) in the array. One might suspect that these quasi-symmetric components are simply result of amplitude calibration errors in our data (dominated by errors on the Ef-Wb baseline). A slight calibration error may arise from the fact that the pointing centre of the VLBI observations was taken from the NASA Extragalactic Database (NED), and it is located about halfway between the eastern and the western VLA components. But this ~ 0.5 arcsecond offset is still small compared to the phased array WSRT beam of 10 arcseconds at 1.6 GHz. We further note that SE and NW are not exactly symmetric around C, and their orientation agrees with both the elongation of the western VLA component, as well as the elongation of the resolved central feature C. However, improved uv -coverage on ~ 100 km baselines is necessary to map better the diffuse emission in this source. In particular, we see a hint of emission in the VLBI data near the eastern VLA component as well, but we cannot reliably image that extended feature since it is almost completely resolved out on VLBI baselines.

The absolute position of the brightest and most compact component C with respect to the assumed J(2000) coordinates of the reference source are $\text{RA} = 17^{\text{h}}01^{\text{m}}24^{\text{s}}.82640$, $\text{Dec.} = +51^{\circ}49'20''.4473$, with an error of about 1 mas. The measured position of component C is about 50 mas offset from the 3σ detection at 8.4 GHz claimed by Blundell & Beasley (1998), and this difference is significant even when we consider the large uncertainties and the fact that different calibrators were used in the two experiments.

The brightness temperature can be estimated with (e.g. Kellermann & Owen 1988):

$$T_{\text{B}} = 1.22 \times 10^{12} (1+z) \frac{S_{\nu}}{\theta^2 \nu_{\text{obs}}^2} \quad (1)$$

where S_{ν} is the measured flux density in Jy, ν_{obs} is the observing frequency in GHz and θ is the angular size in mas. Component C has a brightness temperature of 1×10^8 K, significantly brighter than any other jet components ($\sim 10^6$ K).

4 DISCUSSION

4.1 Identification of the radio core

Earlier it was believed that the radio core was likely hiding in the eastern VLA feature rather than the western one because of its more compact radio morphology on the VLA scales (e.g. Kellermann et al. 1994). The optical position was not accurate enough to exclude the association (Kukula et al. 1998). With our new EVN data this possibility can be firmly excluded since component E is significantly resolved. The nature of component E is not clear. A possible explanation is a residual hot spot in the fading lobe, considering the surrounding diffuse emission.

Another possible location of the radio core is in the western jet feature. Both the VLA and EVN images reveal an elongated jet. The central component C exhibits much more compact morphology and higher brightness temperature than any other components. When compared with the VLA flux density $\sim 0.8 \text{ mJy beam}^{-1}$ at 8.4 GHz and assuming no large variability over 22 years, it has a spectral index of ~ -0.5 ($S_{\nu} \propto \nu^{\alpha}$). This is less steep than the total flux density spectrum: $\alpha \sim -1$ (Barvainis & Lonsdale 1996). If it indeed has a steep spectrum, this is not surprising in radio-weak AGNs, in particular Seyfert nuclei (e.g. Orienti & Prieto 2010; Kharb et al. 2010). Compared with the later VLA observations with the same configuration by Kukula et al. (1998) on 1992 December 11, the total flux density is quite stable in component E, while, a factor of 1.7 lower in component W. Such large change is likely associated with the central AGN activity. Note that this variation is too large ($>10\%$) to be explained as a result of the higher phase errors when the phase self-calibration is not possible. The central compact component is also close to the X-ray counter part detected recently by *XMM-Newton* (Ballo et al. 2011) at $\text{RA} = 17^{\text{h}}01^{\text{m}}24^{\text{s}}.8$, $\text{Dec.} = +51^{\circ}49'20''$ (J2000) and *Chandra* (ObsID 11853) at $\text{RA} = 17^{\text{h}}01^{\text{m}}24^{\text{s}}.7$, $\text{Dec.} = +51^{\circ}49'21''.1$ (J2000). The smoothed *Chandra* X-ray image shows a hint on a jet-like extension, spatially coincident with the jet structure observed in component W. Therefore, the component C is the radio core, indicating the location of the AGN.

The radio core has a brightness temperature slightly lower than other VLBI-detected BAL quasars (e.g. $10^9 - 10^{10}$ K, Liu et al. 2008), but it is at the proper level considering the possible free-free absorption at low frequencies and the large jet viewing angle (see Sect. 4.2). While the overall spectral index of C is still steep (i.e. not showing the inverted spectrum expected for free-free absorption), one should carefully align multi-frequency images at high resolution in the future, to properly image the spectral index distribution within the core. The large difference between

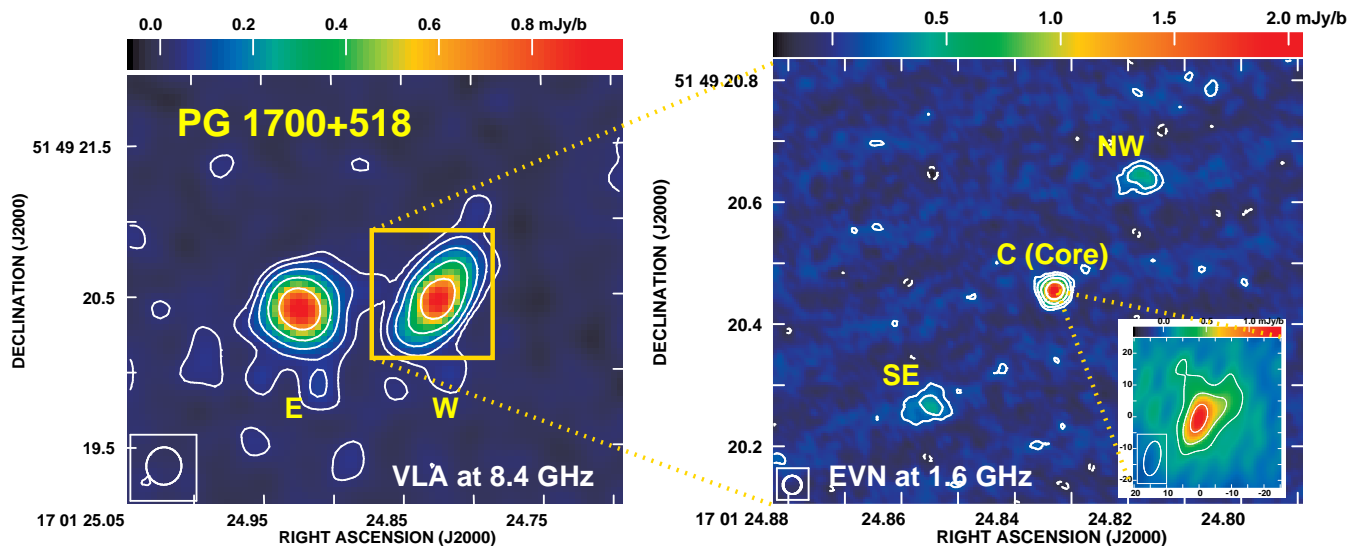


Figure 1. The VLA and EVN intensity images of PG 1700+518. The golden rectangle in the left VLA image shows the field of the right EVN image. The bottom-right inset panel in the EVN image exhibits the inner substructure of component C (core). The contours start from 3σ off-source noise level (VLA: $0.036 \text{ mJy beam}^{-1}$, EVN: $0.15 \text{ mJy beam}^{-1}$) and increase by a factor of 2.

the VLBA (Blundell & Beasley 1998) and our current EVN measurements indicates that either the 3σ VLBA detection was an artifact, or there is indeed a large offset between the two frequencies, and the real radio core is heavily free-free absorbed at 1.6 GHz.

The AGN origin of component C is further strengthened by its high radio luminosity ($1.9 \times 10^{39} \text{ erg s}^{-1}$) which is ~ 100 times higher than the brightest supernovae and SNR. We further note that the ratio of the core radio luminosity to the X-ray luminosity of this source ($2.5 \times 10^{42} \text{ erg s}^{-1}$; Ballo et al. 2011) is $L_R/L_X = 0.76 \times 10^{-3}$, significantly higher than the $L_R/L_X \sim 10^{-5}$ ratios observed in radio quiet quasars (Laor & Behar 2008).

The quasar shows a strong and broad Mg II absorption line at ejection velocities between 7000 and 18000 km s^{-1} (Pettini & Boksenberg 1985). Assuming a viewing angle of 45° (c.f. Sect. 4.2), we can give a lower limit of the jet speed: $0.1c$, where c is light speed. As the core has a low brightness temperature and the two-sided jet components have similar flux density, size and angular separation from the core, the jet is most likely non-relativistic, as found in most Seyfert galaxies (Middelberg et al. 2004).

It is pointed out by Evans et al. (2009) that PG 1700+518 may have significant jet activity as the star-formation rate derived from radio luminosity is a factor of 13 higher than that from the infrared luminosity. This explanation is now confirmed in view of our finding of a radio core with two-sided jet, and a possible large-scale hot spot (component E in the VLA map). The star-forming activity in PG 1700+518 is likely boosted by the interaction with the nearby companion galaxy. Moreover, there may be an extra contribution from jet-induced star-formation. There is a bright infrared knot at a radius ~ 1 arcsec (4.2 kpc) and position angle $\sim 144^\circ$ (Márquez et al. 2003; Stockton et al. 1998). The detection of the knot is significant in the deconvolved H-band image (private communication with I. Márquez). We note that the IR knot (indication of a star-forming region) is right along the jet direction. One may

speculate that the jet interacts with the interstellar medium near component SE and then bends toward North-East, as indicated by the extended emission (VLA component E). However at present we have no firm evidence for this scenario and future high sensitivity observations (also in terms of brightness temperature) are needed to confirm the possibility.

4.2 Similarities with polar-scattered Seyfert 1 Galaxies

The quasar PG 1700+518 is a Seyfert 1-like object within the framework of the unified AGN model since it has broad emission lines. Interestingly, its jet is not as close to the line of sight as in most broad line quasars because the jet components on both sides of the core have been detected with similar total flux density, size and angular separation from the core. This quasi-symmetric jet morphology is typically not found in BAL quasars (e.g. Liu et al. 2008; Jiang & Wang 2003). The jet axis, revealed by our observations, is perpendicular to the polarisation position angle ($55 \pm 4^\circ$, e.g. Schmidt & Hines 1999) of the optical continuum observations. In other words, the scattering plane is along the jet direction. Similar geometry is observed in most Seyfert 2 galaxies and only in around a quarter of Seyfert 1 galaxies. This is broadly explained as a result of a polar scattering region above the accretion disc. These polar-scattered Seyfert 1 galaxies represent the transition between Type 1 and 2 Seyfert galaxies within the model of both polar and equatorial scattering regions (Smith et al. 2004; Axon et al. 2008). By analogy to the classification of Seyfert galaxies, PG 1700+518 has a nucleus resembling polar-scattered Seyfert 1 galaxies with a jet viewing angle ($\sim 45^\circ$), comparable with the torus opening angle.

The X-ray observations of polar-scattered Seyfert 1 galaxies (Jiménez-Bailón et al. 2008) have recently uncovered a nearly ubiquitous signature, the presence of warm and/or cold ($N_H > 10^{21} \text{ cm}^{-2}$) absorption. In the case

of PG 1700+518, its soft X-ray weakness requires $N_{\text{H}} > 10^{24} \text{ cm}^{-2}$ (Ballo et al. 2011), higher than in most polar-scattered Seyfert galaxies.

Our classification provides an independent support for the wind geometry inferred from the simulation (Young et al. 2007). The polarised H α line profile can be well reproduced when the simulation used an intermediate inclination ($\sim 45^\circ$) and a cylindrical wind geometry rather than other wind geometries, such as a disc-like and rotating equatorial outflow.

5 SUMMARY

With the new EVN observations and public VLA archive data, we present the jet structure of PG 1700+518 on parsec to kilo-parsec scales. We find a compact component with a brightness temperature of $\sim 10^8 \text{ K}$ and identify it as the radio core. The jet components on two sides of the core have similar angular separation from the core, similar size and total flux density, indicating a large viewing angle. The jet axis, observed on scales of $< 1 \text{ kpc}$, is well collimated and perpendicular to the polarisation position angle of the optical continuum emission. Together with the recent report of significant cold absorption in the X-rays, we show that the broad line quasar resembles polar-scattered Seyfert 1 galaxies, also indicating a viewing angle of $\sim 45^\circ$. Our radio observations confirm the earlier finding that the radio emission is dominated by AGN activity and not by star-formation. Furthermore, the apparent alignment of the jet with a bright infrared feature may hint on the presence of jet-induced star-formation in the galaxy.

ACKNOWLEDGMENTS

We thank the anonymous reviewer for his constructive suggestions and Michael Garrett for valuable comments on jet-induced star-formation. T. An thanks the financial support by the Overseas Research Plan for CAS-Sponsored Scholars, the Netherlands Foundation for Sciences (NWO) and the Science & Technology Commission of Shanghai Municipality (06DZ22101). F. Wu thanks the JIVE Summer Student Program. The EVN is a joint facility of European, Chinese, South African and other radio astronomy institutes funded by their national research councils. The National Radio Astronomy Observatory is a facility of the National Science Foundation operated under cooperative agreement by Associated Universities, Inc. This research has made use of the NASA/IPAC Extragalactic Database (NED) which is operated by the Jet Propulsion Laboratory, California Institute of Technology, under contract with the National Aeronautics and Space Administration.

REFERENCES

- Antonucci R.R.J., 1983, *Nat*, 303, 158
 Axon D.J. et al., 2008, *Mem. S.A.It.*, 79, 1213
 Ballo L. et al., 2011, *MNRAS*, 415, 2600
 Barvainis R. & Lonsdale C., 1996, *AJ*, 111, 1431
 Blundell K.M. & Beasley A.J., 1998, *MNRAS*, 299, 165
 Evans A.S. et al., 2009, *AJ*, 138, 262

- Greisen E.W., 2003, in Heck A., ed., *Information Handling in Astronomy: Historical Vistas, Astrophysics and Space Science Library*, Vol. 285, Kluwer, Dordrecht, p. 109
 Helmboldt J.F. et al., 2007, *ApJ*, 658, 203
 Hutchings J.B. et al., 1992, *PASP*, 104, 62
 Jiang D.R. & Wang T.G. 2003, *A&A*, 397, L13
 Jiménez-Bailón E. et al., 2008, *RevMexAA*, 32, 131
 Kellermann K.I. et al., 1994, *AJ*, 108, 1163
 Kellermann K.I. & Owen F.N. 1988, in Verschuur G.L. & Kellermann K.I., ed., *Galactic and Extragalactic Radio Astronomy*, Springer, Berlin, p. 563
 Kharb P. et al., 2010, *ApJ*, 723, 580
 Kukula M.J. et al., 1998, *MNRAS*, 297, 366
 Laor A., & Behar E. 2008, *MNRAS*, 390, 847
 Liu Y. et al., 2008, *MNRAS*, 391, 246
 Márquez I. & Petitjean P., 2003, *RevMexAA*, 16, 135
 Middelberg E. et al., 2004, *A&A*, 417, 925
 Orienti M. & Prieto M.A., 2010, *MNRAS*, 401, 2599
 Petrov L. & Taylor G.B., 2011, *AJ*, 142, 89
 Pettini M. & Boksenberg A., 1985, *ApJ*, 294, L73
 Schmidt M. & Green R.F., 1983, *ApJ*, 269, 352
 Schmidt G.D. & Hines D.C., 1999, *ApJ*, 512, 125
 Shepherd M.C. et al., 1994, *BAAS*, 26, 987
 Smith J.E. et al., 2004, *MNRAS*, 350, 140
 Stockton A. et al., 1998, *ApJ*, 500, L121
 Trump J.R. et al., 2006, *ApJS*, 165, 1
 Wampler E.J., 1985, *ApJ*, 296, 416
 Young S. et al., 2007, *Nat*, 450, 74

This paper has been typeset from a $\text{T}_{\text{E}}\text{X}/\text{L}^{\text{A}}\text{T}_{\text{E}}\text{X}$ file prepared by the author.